Proc. Natl. Acad. Sci. USA
Vol. 89, pp. 9242–9246, October 1992
Biochemistry

Single-stranded nucleic acid helical secondary structure stabilized by ionic bonds: $d(A^+\text{-}G)_{10}$*

(single-stranded helix/ionic bonds/H-DNA stability)

NINA G. DOLINNAYA AND JACQUES R. FRESCO†

Department of Molecular Biology, Princeton University, Princeton, NJ 08544

Communicated by Paul Doty, May 26, 1992

ABSTRACT **We have identified a type of secondary structure for the homopurine oligomer $d(A\text{-}G)_{10}$ below pH 6 in 0.01 M Na^+ that is characterized by intense CD but only minor hypochromicity. The stability of this helix, designated $d(A^+\text{-}G)_{10}$, does not depend on oligomer concentration and increases sharply as ionic strength or pH drops, reaching a maximum at 4.0 (melting temperature, 37°C). The pK_a for the transition, 5.3 at 25°C and even higher with decreasing temperature and $[Na^+]$, is much higher than the intrinsic pK_a values for dA or dG residues. While the dA residues are protonated in the helix, further protonation of the dG residues disrupts it. When observed at 280 nm, melting of the helix first results in hypochromicity due to stacking of extrahelical dG residues with neighboring dA residues. The character and temperature dependence of the CD spectra of the constituent dinucleoside monophosphates indicate minimal chirality and base overlap for the A^+pG sequences in $d(A^+\text{-}G)_{10}$ but left-handed twist with some base overlap for the GpA^+ sequences. The observed properties are best satisfied by a model for an intramolecular helix with limited base overlap, stabilized by ionic bonds between dA residues protonated at N-1 and downstream negatively charged phosphates brought close due to the backbone helical twist, while G_{syn} residues lie external to the helix. This structure could provide additional stabilizing energy for biologically relevant protonated non-B-DNA structures adopted by homopurine·homopyrimidine sequences due to topological stress or specific protein binding.**

The secondary structures of single-stranded homo- and copolynucleotides are known to take two general forms: hairpin turns when the sequence allows for base pairing, as in the helical regions of RNA (1), and helically twisted fluctuating stacks of bases, as in poly(A) and poly(C) (2, 3). We now report another type of helical secondary structure for the nucleic acid single strand that seems to depend primarily on intramolecular ionic bonds between protonated dA residues and the backbone phosphates of the oligomer $d(A^+\text{-}G)_{10}$.

In aqueous solution of moderate ionic strength and neutral pH, $d(A\text{-}G)_{10}$ occurs as a multistranded helical structure stabilized by base stacking and hydrogen bonding between pairs or tetrads of bases (4, 5). This structure undergoes a helix → coil transition at room temperature when the ionic strength drops below ≈0.1 M Na^+ (4). Upon protonation of the dA residues of such single strands at lower pH, a new type of secondary structure stabilized by ionic bonds develops, whose features are elaborated in this report. This type of structure may be biologically relevant because it can contribute to the stabilization of intramolecular DNA triplexes as in H-DNA (6).

The publication costs of this article were defrayed in part by page charge payment. This article must therefore be hereby marked "*advertisement*" in accordance with 18 U.S.C. §1734 solely to indicate this fact.

MATERIALS AND METHODS

Oligonucleotides. $d(A\text{-}G)_{10}$ was synthesized by the phosphoramidite method, deprotected, and ultimately purified by electrophoresis in denaturing 20% polyacrylamide gels to remove the $n - 1$ oligonucleotide. Its homogeneity was confirmed by electrophoresis after 5′-end labeling with ^{32}P, which showed a single band of the correct mobility. The extinction coefficient at 260 nm (ε_{260}) of $d(A\text{-}G)_{10}$ was assumed to be 9500 (per residue) in distilled water, the same as for poly[d(A-G)] (8). d(ApG) and d(GpA) were similarly synthesized and deprotected and were ultimately purified using a reverse-phase C_{18} column. Their ε_{260} was assumed to be 12,900 (per residue). Oligomer (residue) concentrations, c, were determined spectrophotometrically.

Solvents. Buffers between pH 3.0 and 7.0 ± 0.05 were prepared by titrating sodium acetate with acetic acid to a final Na^+ concentration of 0.01 M. In some CD experiments, buffers at a fixed pH were used with higher or lower Na^+ concentration, as indicated.

UV Spectroscopy. Absorption spectra and thermal melting profiles were measured with a computer-driven AVIV 14DS spectrophotometer (AVIV Associates, Lakewood, NJ) equipped with a thermoelectrically controlled cell holder. For melting experiments, spectra were measured between 290 and 230 nm every 2° from 3° to 89°C, and these spectra were used to automatically obtain melting profiles and their derivatives at all wavelengths. Cuvettes with 0.1-, 0.5-, and 1.0-cm pathlengths were used to collect data over a range of oligomer concentration. Each melting profile was measured at least twice.

CD Spectroscopy. CD spectra from 320 to 220 nm between 3° and 70°C were recorded on a computer-driven AVIV 62DS CD spectrometer calibrated with (1*S*)-(+)-10-camphorsulfonic acid (Aldrich) and equipped with a thermostatted cuvette holder whose temperature was adjusted with a circulating bath. The cell compartment was continuously purged with dry N_2. Digitized data obtained every nanometer were corrected for baseline and smoothed by a least-squares polynomial fit up to the third order. CD spectra per mole of monomer are plotted as $\varepsilon_L - \varepsilon_R$ in units of liter·mol^{-1}·cm^{-1}. Each spectrum was an average of at least three scans.

RESULTS

Characteristics of Acid-Induced Conformational Transition. As noted, $d(A\text{-}G)_{10}$ forms a multistranded cooperatively melting structure at neutrality in solution of moderate ionic strength at room temperature (4). However, below pH 6 in 0.01 M Na^+, an acid-induced transition occurs, which is completed near pH 4 at room temperature. While this transition is accompanied by a very large increase in the CD

*This is paper no. 18 in the series entitled "Polynucleotides." Paper no. 17 is ref. 7.

†To whom reprint requests should be addressed.

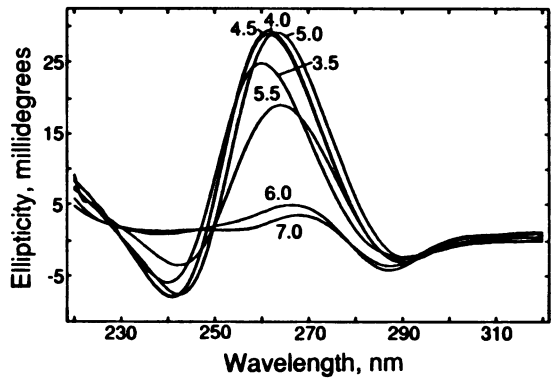

FIG. 1. CD spectra of d(A-G)$_{10}$ at 3°C as a function of pH (pH 3.5–7.0). $c = 0.9 \times 10^{-4}$ M.

spectral intensity, the UV absorption change is minimal. At 3°C, with decreasing pH below 6, there is a dramatic increase in the intensity of the positive band of the CD spectrum, which gradually blue shifts to 261–262 nm at pH 4.0 (Fig. 1). With further lowering of pH, the band intensity drops sharply, so that at pH 3.0, it essentially disappears (see below).

Fig. 2 shows CD-monitored thermal melting profiles of the same solutions. These profiles, even at pH 4.0, which maximally favors the acid-induced conformation, are broader (i.e., less cooperative) than those for the multistranded structure at pH 7 (4). Consistent with the interpretation of Fig. 1, the extent of the conformation at 3°C between pH 4.0 and pH 5.0 is the same, but T_m drops by ≈9°C over this pH range, showing that its stability is very dependent on the extent of residue protonation (see below). At pH 5.5 and above, a decreasing fraction of the oligomer is present as the acid-induced structure at 3°C. Depurination at elevated temperatures prohibits collection of valid melting data below pH 4.

The foregoing effects are better discerned in the CD-monitored titration plots in Fig. 3. Notwithstanding the large positive CD band intensity at pH 4.0, it is striking that the pH-dependent transition is not very sharp, being especially gradual at 25°C (Fig. 3*B*). This is in contrast to the very abrupt acid-induced transitions for poly(A) and poly(C) from single strands to doubly and hemiprotonated duplexes, respectively (9, 10). The unusual nature of the acid-induced transition of d(A-G)$_{10}$ is also apparent from the spectrophotometrically determined pH titration (Fig. 3 *C* and *D*), showing that the absorbance change at $\lambda_{max} = 252$ nm is minimal over the range where the CD change is very large (see also Fig. 4*A*). This difference in UV and CD sensitivity is also in contrast

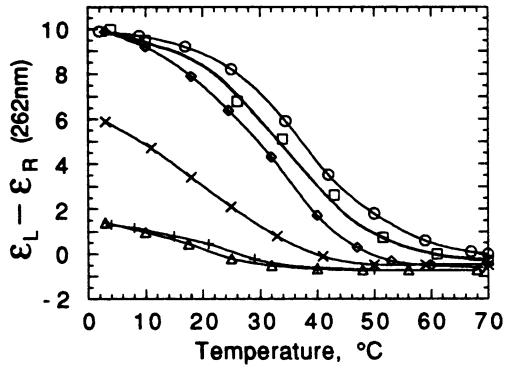

FIG. 2. CD melting profiles of d(A-G)$_{10}$ at pH 4.0 (○), 4.5 (□), 5.0 (◇); 5.5 (×), 6.0 (+), and 7.0 (△).

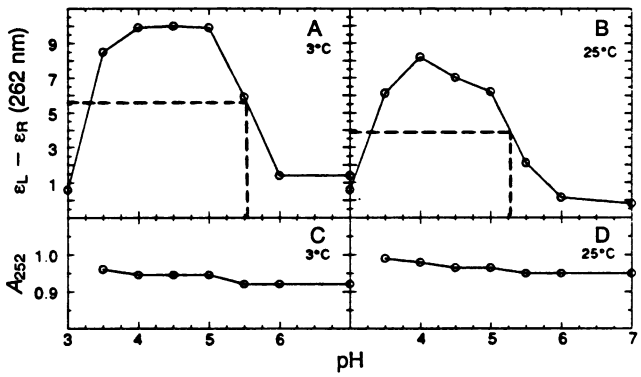

FIG. 3. pH titration curves for d(A-G)$_{10}$ followed by CD (*A* and *B*) and by UV absorption (*C* and *D*). Dashed lines indicate extrapolated pK_a values.

to the parallel CD/ORD and UV changes that accompany the formation of poly(A^+·A^+) and poly(C^+·C) (9, 10).

Titration curves as in Fig. 3 *A* and *B* were used to estimate pK_a values for the acid-induced transition of d(A-G)$_{10}$; in 0.01 M Na^+ the pK_a is 5.30 at 25°C and 5.55 at 3°C, but in 0.001 M Na^+ at 3°C it is ≈0.27 unit higher (data not shown). These values are much higher than those for dGMP (2.9) and dAMP (4.4), showing that a substantial pK_a shift accompanies the conformational transition. The greater proximity of the transition pK_a to the intrinsic pK_a for dA residues suggests that they are the ones protonated in the newly formed structure. This is supported by three other observations. (*i*) The UV spectra for dGMP in protonated and neutral forms are substantially different (Fig. 5*A*), but those for dAMP differ only slightly (Fig. 5*B*), just as is evident in Fig. 4*A* for the oligomer. (*ii*) A comparison of the pH difference spectra for dGMP (Fig. 5*C*), dAMP (Fig. 5*D*), and d(A-G)$_{10}$ (Fig. 4*B*) indicates a strong resemblance between the latter two, with near coincidence of the maxima at 232 and 260 nm, and the minima near 280 nm. By contrast, the corresponding maxima and minima in the dGMP difference spectrum fall near 242, 272, and 292 nm. (*iii*) The precipitous drop in the positive CD band intensity at 262 nm when pH is lowered below 4.0 (Figs. 1 and 3) suggests that protonation of the dG residues leads to disruption of the structure formed maximally at pH 4.0.

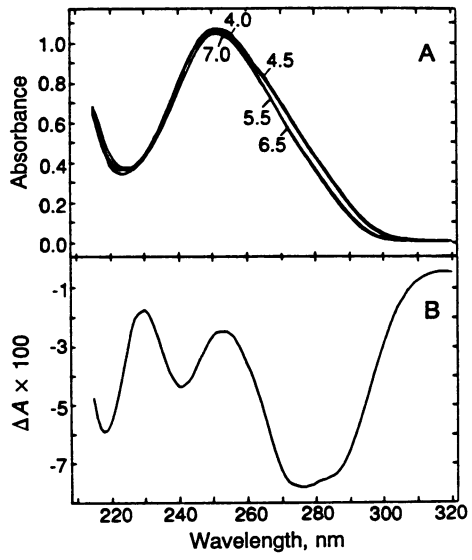

FIG. 4. (*A*) UV absorption spectra of d(A-G)$_{10}$ at 25°C as a function of pH. (*B*) UV difference spectrum between pH 6.5 and pH 4.0.

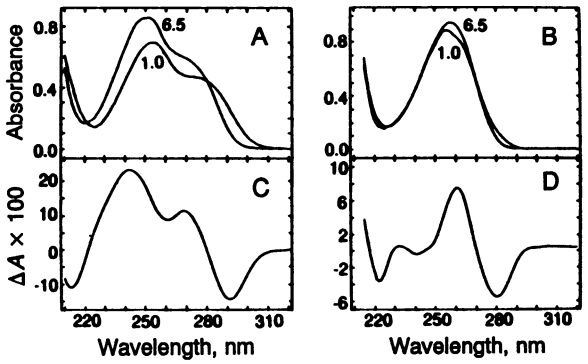

FIG. 5. (*Upper*) UV absorption spectra of 5'-dGMP (*A*) and 5'-dAMP (*B*) at pH 6.5 and pH 1.0 (0.1 M HCl) at 25°C. (*Lower*) UV difference spectra between pH 6.5 and pH 1.0 for 5'-dGMP (*C*) and 5'-dAMP (*D*).

Otherwise, one would expect that this band would plateau or even intensify.

Strandedness of Acid-Induced Conformation. The large shift in the apparent pK_a for the dA residues of the oligomer is consistent with formation of an organized structure to which protonated dA residues make a critical contribution. Thermal melting studies were performed at pH 4.0 over a 12.8-fold range of oligomer concentration in order to distinguish between a single-stranded and a multistranded structure. The four profiles covering this concentration range (Fig. 6) show an absence of concentration dependence of stability, in contrast to that observed for the same oligomer at neutral pH and high ionic strength (4). Also, formation of the acid-induced structure, as well as renaturation of thermally melted $d(A^+\text{-}G)_{10}$, at pH 4.0 occurs fully and instantaneously on cooling (data not shown). Further, the characteristic blue shift that accompanies formation of the protonated parallel-stranded poly(A) duplex (9) is not in evidence in this case.

These observations are consistent with a secondary structure derived from intramolecular interactions, i.e., within a single strand. The interactions could conceivably include base stacking, Coulombic attraction between protonated adenine residues and negatively charged phosphates, or some type of base pairing within hairpin helical turns.

Extent of Base Stacking in $d(A^+\text{-}G)_{10}$. The contrast of high CD intensity and limited hypochromicity for $d(A^+\text{-}G)_{10}$ was further addressed by performing thermal melting studies at pH 4.0 monitored by both methods.

CD and UV spectra between 4° and 50°C (Fig. 7 *A* and *B*) are characterized by prominent isoelliptic and isosbestic points, respectively, suggesting that they represent changing

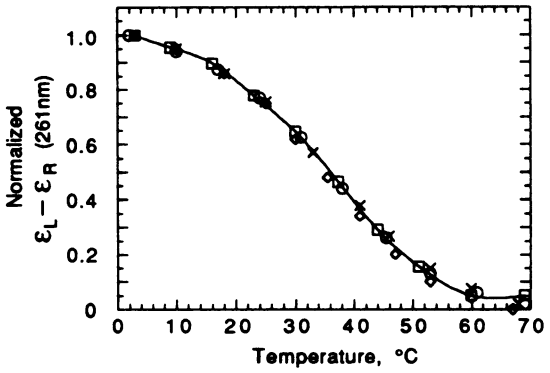

FIG. 6. CD melting profiles for $d(A^+\text{-}G)_{10}$ at pH 4.0 as a function of oligomer concentration. $c = 0.82 \times 10^{-3}$ M (×), 0.22×10^{-3} M (◇), 1.21×10^{-4} M (□), and 0.64×10^{-4} M (○). $\varepsilon_L - \varepsilon_R$ at 3°C is normalized to 1.0.

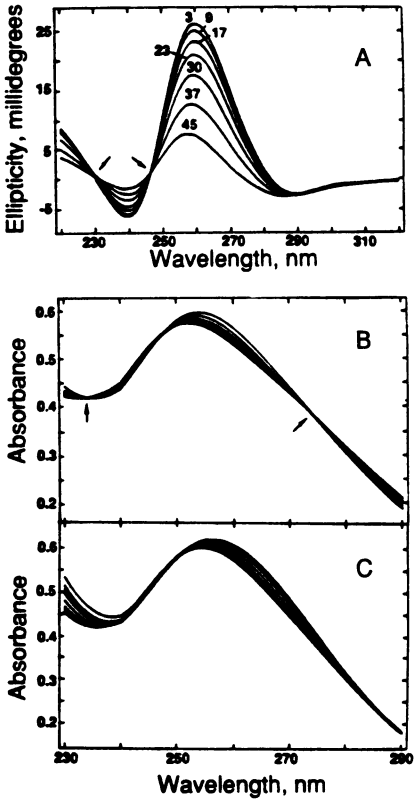

FIG. 7. (*A*) CD spectra for $d(A^+\text{-}G)_{10}$ at pH 4.0 as a function of temperature. $c = 0.77 \times 10^{-4}$ M. (*B* and *C*) UV absorption spectra of $d(A^+\text{-}G)_{10}$ at pH 4.0 between 3° and 45°C (*B*) and between 50° and 90°C (*C*). Spectra were consecutively recorded at 3.6°, 7.6°, 13.6°, 19.6°, 25.6°, 31.6°, 37.6°, and 43.6°C (*B*) or at 49.6°, 55.6°, 61.6°, 67.6°, 73.6°, 83.6°, and 89.6°C (*C*). Note isosbestic and isoelliptic points (arrows).

proportions of two major alternative states over the indicated temperature limits. It is striking that the almost total loss of ellipticity is matched by only a small (9%) hyperchromic change. These observations indicate a conformation for $d(A^+\text{-}G)_{10}$ in which the nucleoside residues are only slightly overlapped but nevertheless manifest the large asymmetry induced by helical order. Hence, the structure cannot contain stacked base pairs as in helical hairpin turns. This is also consistent with the absence of positive ionic-strength dependence of melting at pH 4.0 and our findings that it is not possible to form antiparallel-related A·A base pairs with two hydrogen bonds, and that protonation of all the dA residues contributes to helix stability (data not shown).

Both types of spectra indicate additional conformational changes above 50°C. The CD changes (not shown) are very small, and the spectra no longer pass through the isoelliptic points observable below 50°C. At 55°C, the CD intensity for the oligomer drops to that for d(GpA) at pH 4.0 and 25°C, which corresponds to about the same degree of ionization (see below). Above 50°C, the UV spectra (Fig. 7*C*) constitute a new set of curves with no well-defined isosbestic points.

The distinction between melting below and above 50°C is especially evident in the UV melting profile at 280 nm (Fig. 8), which shows a hypochromic change up to 50°C, followed by a hyperchromic change at higher temperatures. Thus, with increasing temperature up to 50°C, the helical structure of $d(A^+\text{-}G)_{10}$ is gradually disrupted, thereby enabling stacking of nearest-neighbor dA and dG residues that were not stacked and therefore not paired in the helix, showing that the dG residues are essentially extrahelical in that structure. With increasing pH, the temperature at which the profile at 280 nm changes direction drops (data not shown). Once the helix is

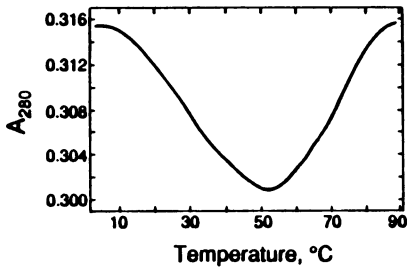

FIG. 8. UV melting profile for $d(A^+\text{-}G)_{10}$ at pH 4.0 monitored at 280 nm.

totally disrupted, hyperchromicity accompanies further temperature increase due to the usual thermal disruption of stacked bases. The clarity with which the melting profile at 280 nm shows these two effects is due to the fact that this wavelength is isosbestic for the unstacking of A residues (11) but is sensitive to stacking of G residues.

Source of Coulombic Attractions in $d(A^+\text{-}G)_{10}$. With the dG residues extrahelical, a requirement for protonated dA residues, and an absence of A·A base pairing, the source of helix stability must reside in some type of dA–backbone interaction, mediated or facilitated by the protonated bases. To confirm this possibility, the ionic-strength dependence of melting of $d(A^+\text{-}G)_{10}$ was studied both at the pH of maximum stability and near the pK_a for the conformational transition. CD melting data at pH 4.0 spanning the Na^+ concentration range 0.0004–0.1 M reveal no detectable impact on the melting profile over this 250-fold range (data not shown). Given the requirement for acid stabilization of the helix, the absence of a counter-ion effect on T_m seems puzzling until it is recognized that at the pH of maximum stability for $d(A^+\text{-}G)_{10}$, which is so far below the apparent pK_a of the dA residues, their degree of protonation is complete and so cannot be modulated by variation in ionic strength. Near the pK_a for the transition, however, the fraction of protonated dA residues is clearly influenced, as anticipated from the effect of ionic strength on the apparent pK_a noted in connection with the titration experiments. Thus, at pH 5.2, T_m rises from ≈0°C in 0.01 M Na^+ to 14.5°C in 0.001 M Na^+; i.e., an inverse dependence on ionic strength is observed.

CD Spectra of d(ApG) and d(GpA). To gain insight into the chiral nature of the elements of the acid-induced helix, the CD spectra of the constituent dinucleoside monophosphates d(ApG) and d(GpA) were examined. In contrast to $d(A^+\text{-}G)_{10}$, the intensities are very low between pH 7 and 1.5. Down to pH 3.5, the spectra for the two dinucleoside monophosphates are quite different (Fig. 9). The spectra converge as pH drops further and both residues become protonated, which must lead to disruption of any base stacking due to repulsion of nearest-neighbor positive charges. In fact, the CD spectra for the dinucleoside monophosphate with both dA and dG residues protonated are quite similar to those in 80% methanol (Fig. 9), where both bases of each dinucleoside monophosphate must also be totally unstacked, in this case due to solvation. In aqueous solution, as the pH rises, the dG residues are first deionized, and some base stacking is manifest at low temperature. Given that base stacking differs for sequence isomers, it is not surprising that the CD spectra for d(ApG) and d(GpA) differ above pH 3.5. However, these spectra differ much more than would be expected if the sense of twist and the conformation about the glycosyl bonds (*syn* vs. *anti*) were the same in the two dinucleoside monophosphates, which has been suggested (12, 13). Thus, as can be seen in Fig. 9*A*, the spectrum for d(ApG) at pH 4 and 3°C is not all that different from that at high temperature, which, in turn, resembles that in 80% methanol. Hence, the bases in d(ApG) are largely unstacked even at low temperature. The comparable CD spectrum of d(GpA) shows well-defined negative and positive bands whose sign is inverted relative to those of right-handed di- or oligonucleotides (14), suggesting a left-handed twist in the stacked neutral and monoprotonated forms.

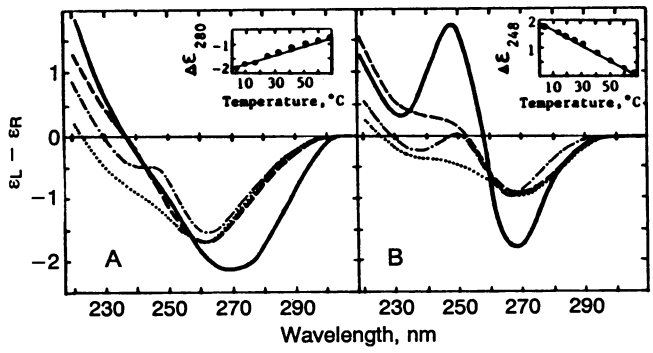

FIG. 9. CD spectra of d(ApG) (*A*) and d(GpA) (*B*) at pH 4.0 and 3°C (—), pH 4.0 and 67°C (– – –), and pH 1.5 (—) or in 80% methanol (····) at 3°C. (*Insets*) Temperature dependence of CD at pH 4.0.

pK_a values for the residues of the two dinucleoside monophosphates determined by UV titration (data not shown) are very close to those for the monomers, in contrast to their substantial upward displacement in $d(A\text{-}G)_{10}$.

In sum, the two constituent dinucleoside monophosphates $d(A^+pG)$ and $d(GpA^+)$ differ in the way they stack and twist about the phosphodiester bond when they are ionized as in the $d(A^+\text{-}G)_{10}$ helix.

DISCUSSION

Single-Stranded vs. Multistranded Structures. That the repeating sequence $d(A\text{-}G)_n$ undergoes some type of acid-induced conformational transition was first noted by Antao *et al.* (15). However, they only characterized the structure as a "self-complex," suggesting its identity with the multistranded structure described by Lee *et al.* (5, 16) at higher ionic strength near neutrality, and that the structure could be induced by either lowering the pH or raising the salt concentration.

In fact, our observations on $d(A\text{-}G)_{10}$ as a function of pH and ionic strength allow us to clearly distinguish between two types of helical structure, a *multistranded* one stabilized by charge-neutralizing ions that does not require protonation of dA residues (4) and the intramolecular *single-stranded* one that has been characterized in this report. Although both structures manifest intense CD, their CD spectra (Fig. 10) are clearly different.

Model for Acid-Induced Helix. In the absence of base pairing or substantial base overlap, the single-stranded helical structure is viewed as being stabilized by ionic bonds between dA residues protonated at N-1 and downstream

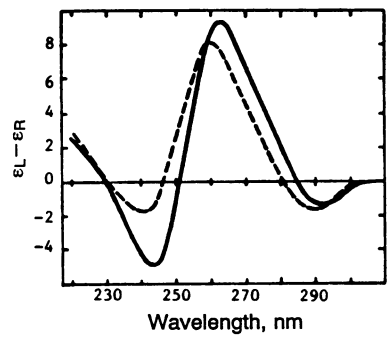

FIG. 10. CD spectra of $d(A\text{-}G)_{10}$ at 25°C in 0.005 M $MgCl_2$/0.05 M Mes, pH 6.0 (—) and in 0.01 M sodium acetate, pH 4.0 (– – –).

negatively charged phosphates brought in proximity by the helical twist of the backbone. Thus, at the pH of maximum stability, essentially all dA residues are protonated (data not shown); also, as the ionic strength is decreased, both pK_a for the transition to the structure and T_m for the helix are raised in proportion to its influence on the degree of protonation of the dA residues.

The marked difference in the CD behavior of the constituent dinucleoside monophosphates suggests that the basic repeating element of the alternating-sequence oligomer is the dinucleotide d(A^+pGp), with dA^+p and dGp in very different conformations. Such nonequivalence has its parallel in Z-DNA, where the overlaps in d(GpC) and d(CpG) segments, with dG in the *syn* orientation, differ markedly (17). Extrapolating further from the conformational features deduced for d(ApG) and d(GpA) to $d(A^+\text{-}G)_{10}$, we presume that the protonated dA residues, which are probably a direct element in the helix, do not overlap their 3′ dG nearest neighbors but overlap slightly with their 5′ dG neighbors with a left-handed sense of twist. This may result in all dG residues lying largely external to the helix. As the *syn* conformation is especially favorable for eliminating stacking of purines with their 5′ neighbors (18), this conformation seems likely, which is also in keeping with the unusual disposition of guanosine residues to take up the *syn* orientation (19). This generates an alternating $dA^+_{anti}\text{-}dG_{syn}$ arrangement along the backbone.

It is not possible at this time to specify the general sense of helical twist or to otherwise better define the structure of $d(A^+\text{-}G)_{10}$. The model is nevertheless sufficient to explain how, in the absence of base pairing and with very limited base overlap, it is possible to generate a helically constrained regular chain with such restriction on the residues that intense CD is induced in their near-UV chromophores.

Biological Relevance. The sequence $d(A\text{-}G)_n\cdot d(C\text{-}T)_n$ occurs often in or near transcriptional regulatory elements, recombinational hotspots, and origins of replication in eukaryotic genomes, and there is much evidence that they adopt various non-B-DNA structures that are especially stabilized by topological stress and acidic pH (20). Until now, the pH effect was attributed to protonation of dC residues, which leads to $C^+\cdot G\cdot C$ base triplets required for formation of intramolecular triplexes of the H-DNA type, while the liberated homopurine sequence was thought to remain single-stranded and devoid of secondary structure. However, it seems energetically unfavorable to maintain a totally unneutralized homopurine backbone segment constrained within the immediate vicinity of the H-DNA triplex segment, which itself is more highly negatively charged than a duplex. The finding that the linear A-G-A-G . . . sequence can assume a stable partially neutralized intramolecular single-stranded helical conformation at pH < 6 suggests that this structure could provide an important source of stabilizing energy for such non-B-DNA structures. This is especially relevant since linear $C^+\cdot G\cdot C$-containing triplexes can occur at pH 7 (7), whereas H-DNA-type structures generally require reduced pH for stability (21). While there are counterarguments that structures requiring less than physiological pH are not of biological relevance, the fact that the intramolecular $d(A^+\text{-}G)_n$ helix can exist means that a protein which recognizes it will, upon binding, stabilize it and thereby raise the pK_a for the required protonation. Proteins that bind to the single-stranded homopurine element of H-DNA have been reported (22, 23); so have DNA-binding proteins with acidic domains (24) that can create an acidic environment in the immediate vicinity of DNA. Hence, there are a number of ways that the combined effects of topological stress and protein binding could cooperate to make the secondary structure described here operative in the cell. Finally, we note that this type of secondary structure is conceivable for any constrained purine-rich single-strand segment with a substantial fraction of dA residues.

This work was supported by grants from the National Institutes of Health (GM42936) and the National Science Foundation (DMB8419060).

1. Fresco, J. R., Alberts, B. M. & Doty, P. (1960) *Nature (London)* **188**, 98–101.
2. Leng, M. & Felsenfeld, G. (1966) *J. Mol. Biol.* **15**, 455–466.
3. Adler, A., Grossman, L. & Fasman, G. D. (1967) *Proc. Natl. Acad. Sci. USA* **57**, 423–430.
4. Shiber, M. C., Braswell, E. H., Dolinnaya, N. G., Friedman, R., Kim, Y. J., Klump, H., Mukherjee, I., Spiro, T. G. & Fresco, J. R. (1993) *Nucleic Acids Res.*, in press.
5. Lee, J. S. (1990) *Nucleic Acids Res.* **18**, 6057–6060.
6. Frank-Kamenetskii, M. D. (1990) in *DNA Topology and Its Biological Effects*, eds. Cozzarelli, N. R. & Wang, J. C. (Cold Spring Harbor Lab., Cold Spring Harbor, NY), pp. 185–215.
7. Letai, A. G., Palladino, M. A., Fromm, E., Rizzo, V. & Fresco, J. R. (1988) *Biochemistry* **27**, 9108–9112.
8. Lee, J. S., Evans, D. H. & Morgan, A. R. (1980) *Nucleic Acids Res.* **8**, 4305–4320.
9. Fresco, J. R. & Klemperer, E. (1959) *Ann. N.Y. Acad. Sci.* **81**, 730–741.
10. Guschlbauer, W. (1967) *Proc. Natl. Acad. Sci. USA* **57**, 1441–1448.
11. Fresco, J. R., Klotz, L. C. & Richards, E. G. (1963) *Cold Spring Harbor Symp. Quant. Biol.* **28**, 83–90.
12. Cantor, C. R., Warshaw, M. M. & Shapiro, H. (1970) *Biopolymers* **9**, 1059–1077.
13. Warshaw, M. M. & Cantor, C. R. (1970) *Biopolymers* **9**, 1079–1103.
14. Ikehara, M., Vesugi, S. & Yano, J. (1972) *Nature (London) New Biol.* **240**, 16–17.
15. Antao, V. P., Gray, D. M. & Ratliff, R. L. (1988) *Nucleic Acids Res.* **16**, 719–738.
16. Lee, J. S., Johnson, D. A. & Morgan, A. R. (1979) *Nucleic Acids Res.* **6**, 3073–3091.
17. Wang, A. H.-J., Quigley, G. J., Kolpak, F. J., van der Marel, G., van Boom, J. H. & Rich, A. (1980) *Science* **211**, 171–176.
18. Olson, W. K. (1973) *Biopolymers* **12**, 1787–1814.
19. Guschlbauer, W., Friĉ, I. & Holý, A. (1972) *Eur. J. Biochem.* **31**, 1–13.
20. Wells, R. D., Collier, D. A., Hanvey, J. C., Shimizu, M. & Wohlrab, F. (1988) *FASEB J.* **2**, 2939–2949.
21. Shimizu, M., Hanvey, J. C. & Wells, R. D. (1990) *Biochemistry* **29**, 4704–4713.
22. Davis, T. L., Firulli, A. B. & Kinniburgh, A. J. (1989) *Proc. Natl. Acad. Sci. USA* **86**, 9682–9686.
23. Hoffman, E. K., Trusko, S. P., Murphy, M. & George, D. L. (1990) *Proc. Natl. Acad. Sci. USA* **87**, 2705–2709.
24. Ptashne, M. (1988) *Nature (London)* **335**, 683–689.